SEMARAK ILMU PUBLISHING

CFD Letters

Journal homepage:
https://semarakilmu.com.my/journals/index.php/CFD_Letters/index
ISSN: 2180-1363

Investigating the Effects of Vortex Generator Geometry on NACA Inlet Performance

Rinal Kharis[1], Harinaldi[1*]

[1] Department of Mechanical Engineering, Faculty of Engineering, Universitas Indonesia, Depok 16424, Indonesia

ARTICLE INFO

Article history:
Received 13 December 2023
Received in revised form 15 January 2024
Accepted 17 February 2024
Available online 31 August 2024

Keywords:
NACA Inlet; flow control; vortex generator; ram recovery ratio; mass flow ratio

ABSTRACT

The NACA inlet is a submerged inlet that is widely used in aviation. It has the advantages of low drag and low radar cross-section. One of the considerations in using the NACA inlet is the low-pressure recovery compared to other types of inlets. To improve the pressure recovery of the NACA inlet, it can be done by controlling the boundary layer thickness in the upstream of the NACA inlet. This study aims to investigate the effect of the use and geometric parameters of vortex generators on the improvement of the performance of the NACA inlet. The geometric parameters that will be varied are height, angle of incidence, and distance between vortex generators. Various configurations will be simulated numerically with ANSYS Fluent using the k-ω SST turbulence model. The results indicate that the use of vortex generators can increase the Ram recovery ratio by 31.23% and the Mass flow ratio by 14.74%. The most effective vortex generator height to use depends on the local boundary layer thickness. The effective angle of incidence and spacing of the vortex generator were obtained at 20 degrees and 20 mm, respectively. These results indicate that there are effective angles and spacings in the vortex generator configuration to improve the performance of the NACA inlet.

1. Introduction

The inlet is a propulsion system component that provides air for both primary needs and cooling. The submerged inlet is a type of inlet employed in both aircraft and automotive applications, positioned in a recessed manner on the contours of the vehicle with specific wall shapes such as straight, straight divergent, or curved divergent. The working principle of the submerged inlet is to utilize two counter-rotating vortices formed on the wall which draw the freestream flow into the inlet. Due to its low-pressure recovery, the submerged inlet is commonly used for auxiliary needs, such as providing cold air. The NACA inlet is a type of submerged inlet that was developed by the National Advisory Committee for Aeronautics (NACA) in 1945. This inlet has a wall in the form of a divergent curve with certain coordinates. The NACA inlet offers advantages in terms of low drag force [1]. This inlet structure is lighter and has a low radar cross-section.

* *Corresponding author.*
E-mail address: harinaldi.d@ui.ac.id (Harinaldi)

https://doi.org/10.37934/cfdl.17.1.1734

The limitation of the submerged inlet, indicated by its low-pressure recovery, offers an exploitable opportunity for researchers. The performance of the submerged inlet is determined by the thickness of the boundary layer. Thicker boundary layers result in decreased performance of the submerged inlet, thus many studies focus on modifying the flow to reduce the thickness of the boundary layer at the upstream submerged inlet. The parameters commonly used in the evaluation of the submerged inlet performance are the Ram recovery ratio and the Mass flow ratio.

Several studies employ passive flow control methods to enhance the performance of submerged inlets, with vortex generators being a commonly used flow control device. Some research indicates that vane-type vortex generators can decrease the thickness of the boundary layer [2], leading to an improvement in submerged inlet performance of up to 40% [3]. The presence of vortex generators significantly influences the flow structure entering the inlet, resulting in higher total pressure compared to a standard NACA inlet [4]. In the context of using vortex generators for flow control in NACA inlets, the effectiveness of flow control is determined by parameters such as vortex generator height, incidence angle, spacing, and separation point [5]. Additionally, vortex generators are effective only within a specific range of inlet velocity ratios [6]. The most significant placement of vortex generators for reducing boundary layer thickness occurs at the furthest distance from the inlet [7]. The optimal placement of vortex generators is crucial in determining their effectiveness, and the height of the vortex generator is proportional to the thickness of the boundary layer [8].

The use of another flow control method, a ridge-shaped diverter, can enhance pressure recovery with increasing Mach number [9]. A submerged diverter is also capable of directing a significant portion of low-energy flow into the diverter, leading to a thin boundary layer at the submerged inlet [10].

An overview of studies on the application of passive flow control in submerged inlets is presented in Table 1. According to Table 1, there have been relatively fewer studies conducted on NACA inlet types compared to other submerged inlet types. The most commonly used passive flow control is the vortex generator. The research results using vortex generators indicate that influential parameters include height, incidence angle, and spacing between vortex generators.

Table 1
The overview of submerged inlet studies

No	Flow Control	Submerged Inlet	Findings	Reference
1	Vane-type VG	Straight-parallel, NACA,	- Vane-type VG is capable of reducing boundary layer thickness and increasing ram pressure. - Parameters affecting flow control effectiveness are VG height, incidence angle, and spacing.	[2-6]
2	Delta wing VG	NACA	- The farthest horizontal distance from the inlet can significantly reduce boundary layer thickness. - As the incidence angle of the VG increases, the performance of the inlet decreases.	[7]
3	Bump-shaped VG	Straight-parallel	- The optimal placement of VG significantly determines the optimal size of the vortex generator. - The height of the vortex generator is proportional to the thickness of the boundary layer.	[8]
4	Diverter	Straight-divergent	- The ridge diverter can divert the boundary layer and stream tube, improving pressure recovery. - A portion of low-energy flow enters the diverter, leading to a thin boundary layer.	[9, 10]

From a review of studies on the use of passive flow control to enhance the performance of submerged inlets, it is evident that there have been relatively few studies using NACA inlets as their subject, despite NACA inlets being among the best-performing submerged inlets. Passive flow control can be employed as a device to enhance ram pressure recovery from the inlet. Research into improving the performance of NACA inlets is conducted to provide an alternative inlet with performance approaching that of scoop inlets. By achieving performance similar to scoop inlets, an inlet with the advantages of low drag and lighter weight while maintaining good performance can be obtained. Based on these considerations, this study aims to investigate the effect of the use and geometric parameters of vortex generators on the improvement of the performance of the NACA inlet. The parameters that will be varied are height, angle of incidence, and vortex generator spacing. The Ram recovery and Mass flow ratio will be used to determine the performance of the NACA inlet. The study is conducted using a benchmark Medium Altitude Long Endurance (MALE) UAV developed in Indonesia known as Elang Hitam. Elang Hitam uses a scoop inlet for its main intake and cooling. With the alternative use of NACA inlets, it is expected that the aircraft's performance will improve due to a reduction in structural weight and drag.

2. Methodology

2.1 Geometry Modelling and Meshing Generation

The NACA inlet model used in this study, as shown in Figure 1, is designed based on the inlet model studied by Mossman and Randall [11]. The main dimensions of the NACA inlet in this study include an entrance height of 50.8 mm, an entrance width of 203.2 mm, and a ramp angle of 7 degrees. The selected height-to-width ratio is 4, as this ratio is known to yield the best pressure recovery [12]. The vortex generator used is the vane-type vortex generator, as shown in Figure 2(a). The chosen configuration is triangular with a counter-rotating setup, as this type provides a 20% performance improvement compared to other shapes [13]. Moreover, triangular-shaped vortex generators exhibit high turbulent intensity, thereby enhancing momentum transport [14]. The maximum height of the vortex generator will adjust to the local boundary layer thickness [15], with a length of 2 times the height and a width of one-fourth of the height. Theoretically, the boundary layer thickness at the vortex generator position in this study is 64 mm. The vortex generator will be varied according to geometric parameters, as shown in Figure 2(b). In Figure 2(b), the notation *h* represents the height of the vortex generator, *d* indicates the spacing between vortex generators, and β indicates the angle of incidence of the vortex generator.

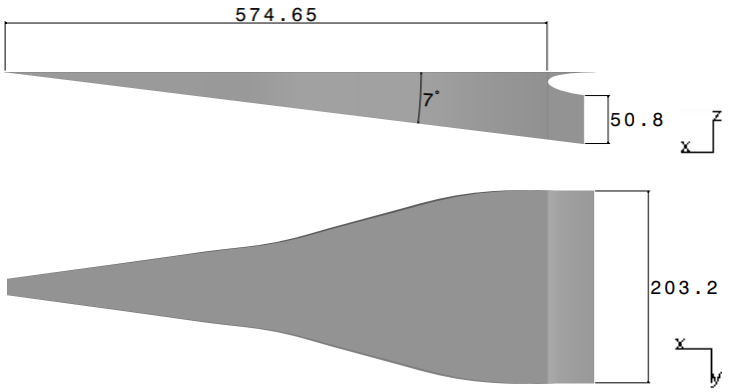

Fig. 1. The geometry model of the NACA inlet (in mm)

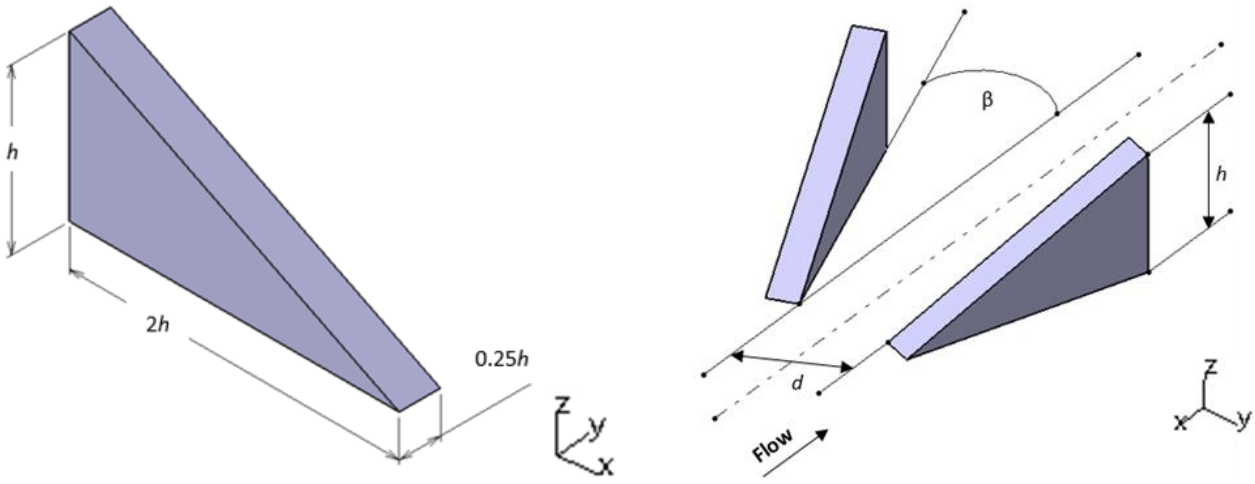

(a) (b)

Fig. 2. The geometry model of Vortex Generator (a) Size (b) VG geometric parameters

The computational domain used in this study is illustrated in Figure 3. The NACA inlet is positioned at 7,000 mm from the inlet position in the computational domain, corresponding to its location on the Elang Hitam fuselage. The total domain length is 10,000 mm, with a height of 1,000 mm and a width of 2,000 mm. The vortex generator will be placed at a position 2,700 mm upstream of the NACA inlet based on our separate research findings. Pressure far-field conditions are applied to the inlet section of the freestream, and pressure outlet conditions are applied to the outlet section of the freestream and duct. The bottom section of the domain, NACA, and duct are defined as walls.

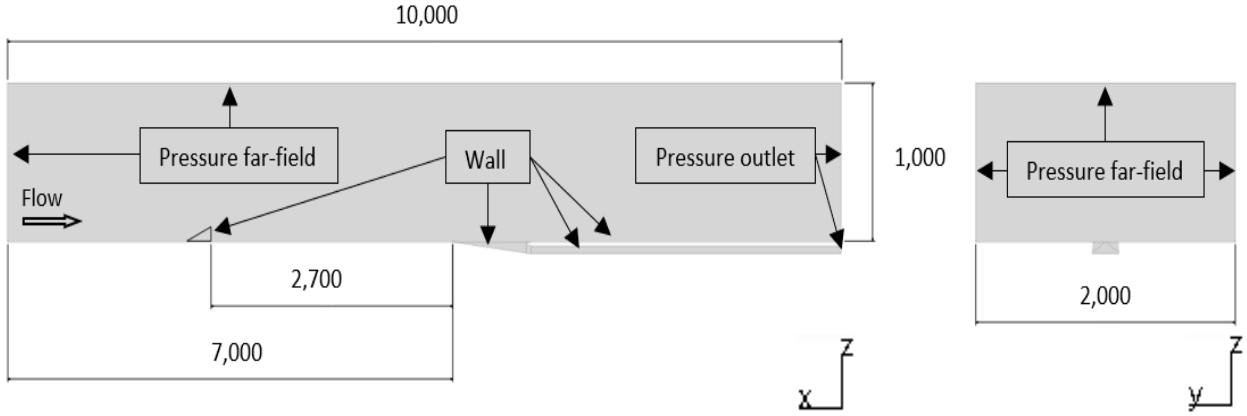

Fig. 3. The domain and boundary condition (in mm)

Meshing was performed on the NACA inlet geometry with a vortex generator and the standard NACA inlet using a hexahedral mesh type. The hexahedral mesh type was chosen for its high accuracy and faster run time [16]. Mesh quality will be evaluated using skewness and orthogonal quality. The mesh for each configuration will be varied for Grid Convergence Index calculations. Figure 4 illustrates the mesh results for the NACA inlet geometry with a vortex generator, comprising 2,125,699 elements.

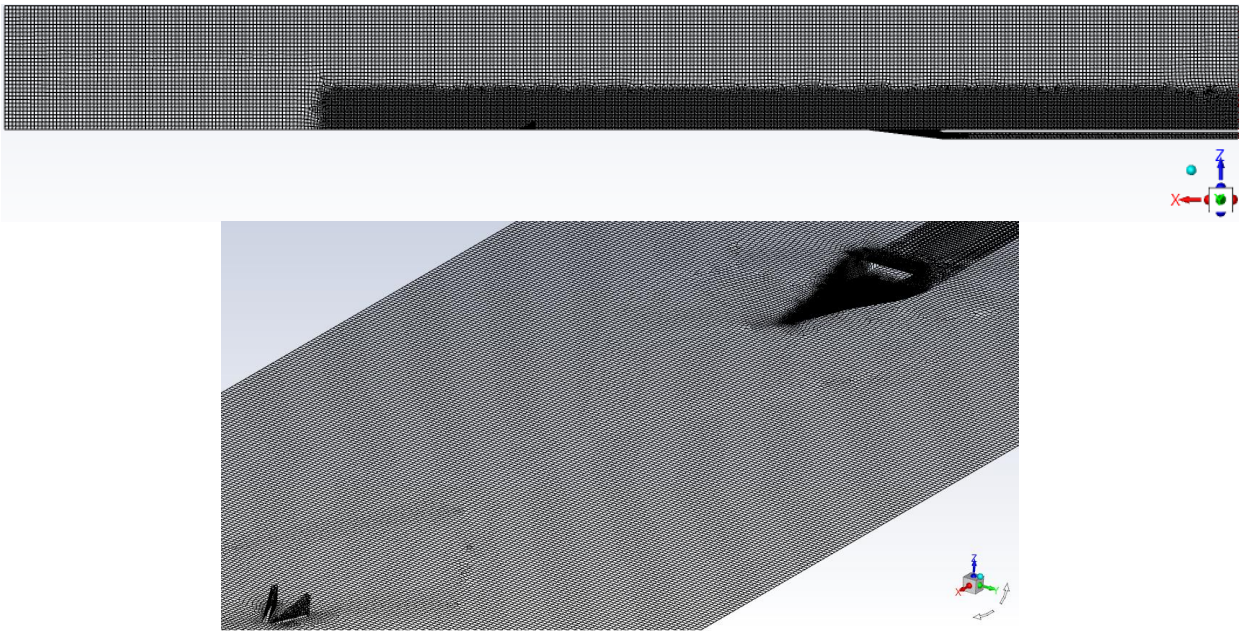

Fig. 4. Mesh of NACA inlet with vortex generator

2.2 Computation Setup and Parameter Study

The flow simulation is conducted using ANSYS Fluent. The RANS equation is solved with the SST k–ω turbulence model to obtain results in a steady-state condition. The SST k–ω turbulence model is used in this study because it provides a combination of strength to capture phenomena in near-wall layers and free-stream regions [17]. In ANSYS Fluent, the SST k-ω model includes those that use Enhanced Wall Function, where this method can extend its applicability throughout the near-wall region and formulate the law-of-the wall as a single wall law for the entire wall region [18]. This indicates that the SST k-ω model is capable of directly resolving viscous layers, and the y+ value does not have an effect. However, in this study, y+ is set in the range of y+ < 500, resulting in approximately 7 mm for the first grid cell. The freestream airflow is modeled as an ideal gas with conditions corresponding to the service ceiling of Elang Hitam at an altitude of 6,000 meters AGL. The freestream flow conditions at an altitude of 6,000 meters are derived from the U.S. Standard Atmosphere data and can be seen in Table 2 [19]. The properties in Table 2 will be used as initial values for the boundary conditions. The average cruise speed of Elang Hitam is 52 m/s, resulting in a Mach number of 0.16432 used in the simulation.

Table 2
Freestream flow condition at 6,000 m

Properties	Value
Pressure	47,217 N/m2
Speed of sound	316.45 m/s
Temperature	219.19 K

The simulation will be conducted according to the cases listed in Table 3 to investigate the influences of geometric parameters. In Table 3, the geometric parameters of the vortex generator will be varied based on height, angle of incidence, and vortex generator spacing. The height of the vortex generator will be varied from 1.0δ (boundary layer thickness) to 0.5δ. The angle of incidence will be varied from 12 to 24 degrees. For vortex generator spacing, variations will be made from 5 to 50 mm.

Table 3
Vortex generator geometric parameters

Configuration	Height, *h* (mm)	Angel of incidence, β (Degree)	Spacing, *d* (mm)
1	64	20	10
2	58	20	10
3	52	20	10
4	45	20	10
5	32	20	10
6	64	12	10
7	64	14	10
8	64	16	10
9	64	18	10
10	64	22	10
11	64	24	10
12	64	20	5
13	64	20	15
14	64	20	20
15	64	20	30
16	64	20	50

To evaluate the simulation results with variations in geometric parameters, two non-dimensional parameters are used. The performance of the NACA inlet will increase with the rise of these parameters. The first parameter is the Ram recovery ratio, which is a primary measure of the performance of the submerged inlet. The Ram recovery ratio is the ratio of dynamic pressure at the duct entrance to freestream flow. In this study, the Ram recovery ratio is defined based on dynamic pressure as per Eq. (1).

$$\eta = \frac{P_{T,1} - P_0}{P_{T,0} - P_0} \tag{1}$$

Where $P_{T,0}$ is the total pressure of the freestream, and $P_{T,1}$ is the total pressure at the duct entrance plane. P_0 is the static pressure of the freestream.

The second non-dimensional parameter is the mass flow ratio. The Mass flow ratio is the ratio of the intake mass flow to the freestream mass flow. The Mass flow ratio is defined according to Eq. (2).

$$MFR = \frac{\dot{m}_1}{\dot{m}_0} = \frac{\rho_1 \cdot V_1 \cdot A_1}{\rho_0 \cdot V_0 \cdot A_1} \tag{2}$$

Where ρ_1 is the density at the duct entrance plane, v_1 is the velocity at the duct entrance plane, and A_1 is the duct entrance plane area. ρ_0 is the density at the freestream, v_0 is the freestream flow velocity.

2.3 Grid Convergence Index and Validation

In CFD simulations, the verification stage is crucial to determine the accuracy of the model implementation. In verification, refining the grid size aims to estimate the discretization error of the numerical solution [20]. One of the methods used for verification is the Grid Convergence Index (GCI). GCI is a method developed to estimate grid convergence error based on Richardson's extrapolation [21]. Two or more progressively finer grids are used to run the simulation as part of the method. To accurately estimate the order of convergence, three levels of grid are recommended.

The first step for GCI is to determine the grid refinement ratio using Eq. (3) as follows.

$$r = \left(\frac{N_{fine}}{N_{coarse}}\right)^{1/d} \tag{3}$$

Where *N* is the number of grid points, *d* is the flow domain. The value of *r* must be greater than 1.1.

The next step is to perform simulation with three grids to obtain the objective value. In this study, ram recovery (η) and mass flow ratio (*MFR*) are the objective values. The order of convergence is determined using Eq. (4) and Eq. (5).

$$p = \frac{1}{\ln(r_{21})} ln \left|\frac{\eta_3 - \eta_2}{\eta_2 - \eta_1}\right| \tag{4}$$

$$p = \frac{1}{\ln(r_{21})} ln \left|\frac{MFR_3 - MFR_2}{MFR_2 - MFR_1}\right| \tag{5}$$

The value of the GCI is determined using the fine-grid convergence index parameters as shown in Eq. (5) until Eq. (9).

$$GCI_{fine}^{21} = \frac{1.25\left|{\eta_1 - \eta_2}/{\eta_1}\right|}{(r_{21}^p - 1)} 100\% \tag{6}$$

$$GCI_{fine}^{32} = \frac{1.25\left|{\eta_2 - \eta_3}/{\eta_2}\right|}{(r_{32}^p - 1)} 100\% \tag{7}$$

$$GCI_{fine}^{21} = \frac{1.25\left|{MFR_1 - MFR_2}/{MFR_1}\right|}{(r_{21}^p - 1)} 100\% \tag{8}$$

$$GCI_{fine}^{32} = \frac{1.25\left|{MFR_2 - MFR_3}/{MFR_2}\right|}{(r_{32}^p - 1)} 100\% \tag{9}$$

To determine whether the solutions were in the asymptotic range of convergence,

$$\frac{GCI_{32}}{r^p \times GCI_{21}} \cong 1 \tag{10}$$

According to Eq. (3) through Eq. (10), the GCI values for the Ram recovery and the Mass flow ratio for the NACA inlet with a vortex generator are presented in Table 4 and Table 5, respectively. The solutions on the two finest grids resulted in values of 0.999 and 0.991 for ram recovery and mass flow ratio, respectively. The solutions on the two finest grids resulted in values close to 1, indicating that they are still within the asymptotic range of convergence. Based on the GCI study, the error values for Ram recovery and Mass flow ratio are estimated to be 0.003% and 3.062%, respectively. In the next study with a different configuration, an approximate element size of 2 million will be used.

Table 4
Grid convergence index calculation for ram recovery ratio

Symbol	Value
N_1	3,962,274
N_2	2,129,131
N_3	1,037,512
η_1	0.7806
η_2	0.7812
η_3	0.7583
r_{21}	1.2300
r_{32}	1.2708
p_{21}	17.583
p_{32}	15.191
GCI_{21}	0.003%
GCI_{32}	0.099%
Range	0.999

Table 5
Grid convergence index calculation for mass flow ratio

Symbol	Value
N_1	3,962,274
N_2	2,129,131
N_3	1,037,512
MFR_1	0.7133
MFR_2	0.7197
MFR_3	0.7110
r_{21}	1.2300
r_{32}	1.2708
p_{21}	1.4977
p_{32}	1.2940
GCI_{21}	3.0615%
GCI_{32}	4.1376%
Range	0.991

A mesh size of 2 million elements was also used for the standard NACA inlet to obtain the values of Ram recovery and Mass flow ratio. These two parameter values will be used as a comparison with the NACA inlet with vortex generator. Simulation results for the standard NACA inlet with variations in velocity ratio at a freestream flow altitude of 6,000 m are shown in Figure 5. These results are compared with experimental results from the NACA Report of 1948 [11]. The simulation results exhibit a trendline that closely resembles the experimental results. The difference in the Ram recovery ratio values between the simulation results and experimental data is attributed to the difference in total pressure values. Pressure values in the simulation are based on conditions at an altitude of 6,000 m, while the experimental results were conducted at sea level conditions. This is also consistent with the findings of Li *et al.,* [22] who revealed that an increase in altitude leads to a decrease in total pressure at the engine intake.

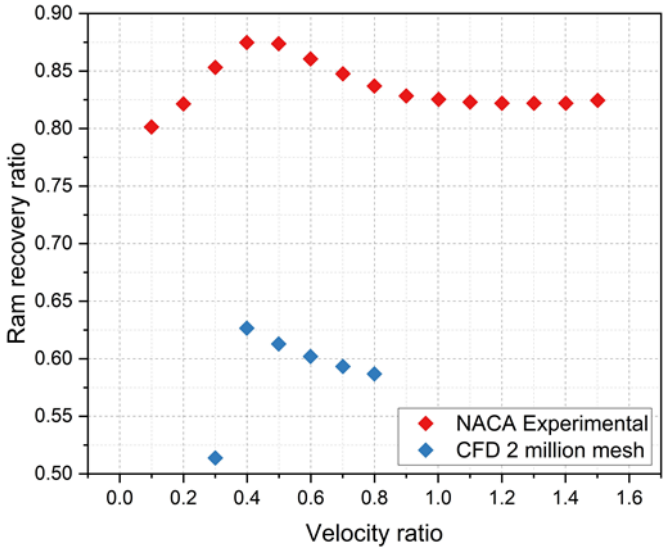

Fig. 5. Ram recovery as a function velocity ratio for the Standard NACA inlet and experimental data

3. Results

3.1 Standard NACA Inlet

The simulation conducted on the standard NACA inlet shows a Ram recovery ratio of 0.5953 and a Mass flow ratio of 0.6272. Both values will be used as a comparison with the simulation results for the NACA inlet with a vortex generator. The Streamline as shown in Figure 6 illustrates the flow within the NACA inlet. It is observed in the figure that only a portion of the freestream flow enters the inlet, while the rest bypasses the inlet. In the duct, a swirl flow is formed due to the flow passing through the curved walls of the inlet.

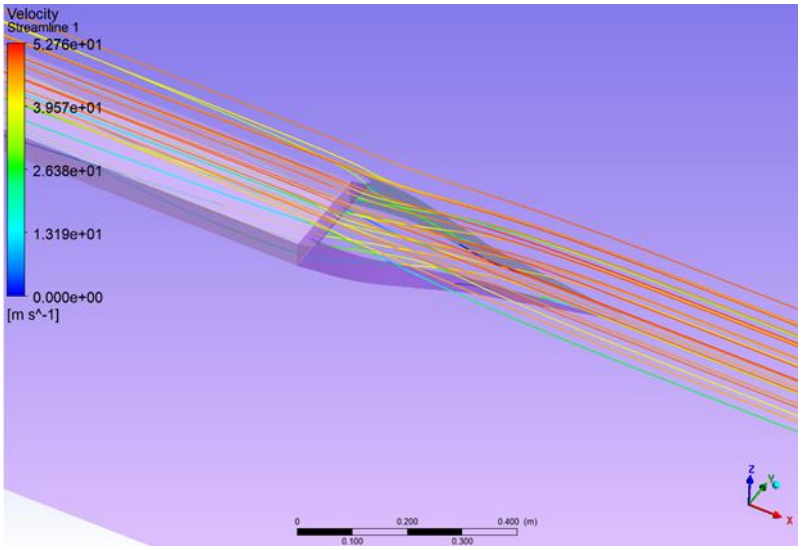

Fig. 6. Streamline in standard NACA inlet

The parameter indicating the performance of the NACA inlet is the boundary layer thickness. The thicker the boundary layer, the lower the performance of the NACA inlet. The boundary layer configuration for the standard NACA inlet is presented in Figure 7. At the initial section plane of the NACA inlet, the flow entering the inlet is unaffected by the inlet walls, resulting in a boundary layer thickness identical to the surface wall. In the middle section plane, it is observed that the boundary

layer thickness on the ramp decreases because the curved inlet walls generate vortices capable of redirecting freestream flow into the inlet. This can also be observed in Figure 8, where the inlet walls form vortices to direct freestream flow into the inlet and sweep the boundary layer.

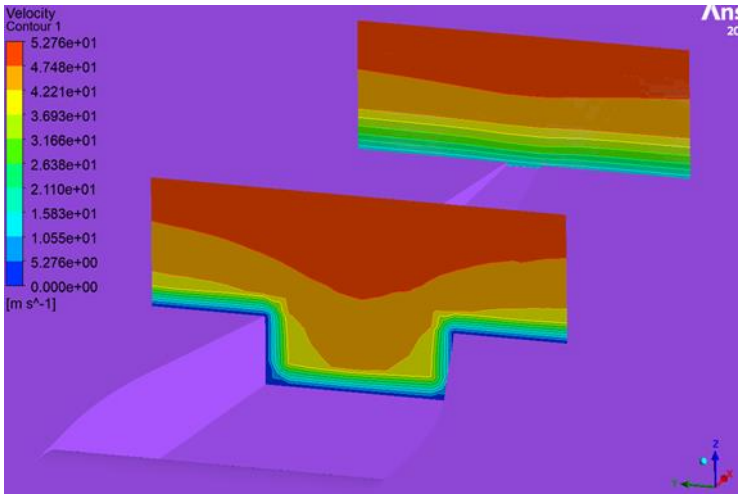

Fig. 7. Velocity contour in standard NACA inlet

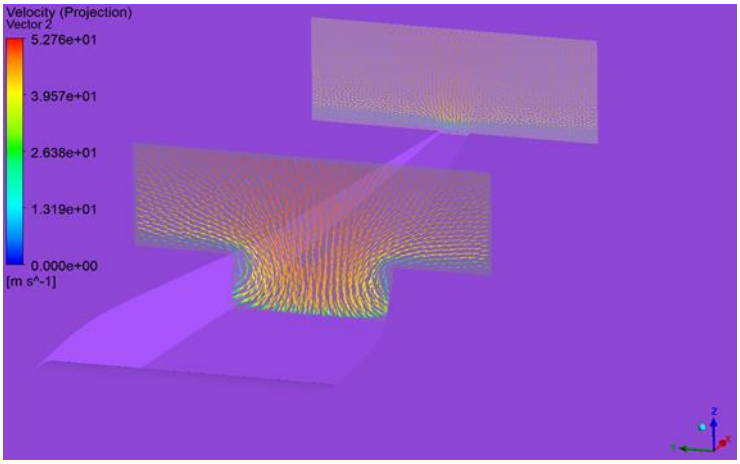

Fig. 8. Velocity vector in standard NACA inlet

3.2 Effect of Vortex Generator Height

The first geometric parameter of the vortex generator to be varied is the height of the vortex generator. Simulations for varying the height of the vortex generator were conducted with a configuration of a 20-degree angle of incidence and a 10 mm spacing between vortex generators, featuring five variations in the height range from 32 mm (0.5δ) to 64 mm (1.0δ). The simulation results for Ram recovery ratio are shown in Figure 9(a). The height of the vortex generator has a significant impact on improving the performance of the NACA inlet. Figure 9(a) clearly shows that the higher the vortex generator, the greater the value of the Ram recovery ratio. The highest Ram recovery ratio is achieved in the configuration with a height of 64 mm, with a ratio value of 0.77878. This value indicates an increase of 30.83% compared to the Ram recovery ratio of the standard NACA inlet. The results for the mass flow ratio parameter, as shown in Figure 9(b), also exhibit a similar trend to the Ram recovery ratio. With an increase in the height of the vortex generator, the mass flow ratio value tends to rise. The highest Mass flow ratio achieved at a vortex generator height of

64 mm is 0.71738. This Mass flow ratio value increases by approximately 14.37% compared to the standard NACA inlet value.

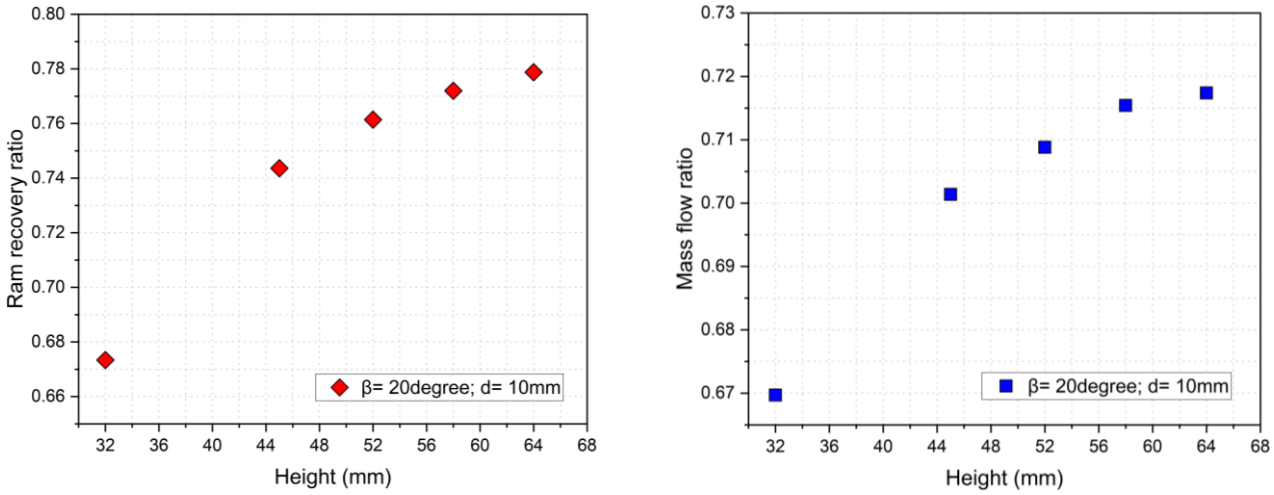

(a) (b)

Fig. 9. Effect of vortex generator height (a) Ram recovery ratio (b) Mass flow ratio

The use of a vortex generator in the NACA inlet will reduce the boundary layer thickness, leading to an increase in the Ram recovery ratio and Mass flow ratio. Figure 10 shows a comparison of velocity contours at the end section plane between the NACA inlet with a vortex generator and the standard NACA inlet. It can be observed that the NACA with a vortex generator has a thinner boundary layer compared to the standard NACA inlet. The reduction in boundary layer thickness affects the flow in the duct entrance region. Figure 11 displays a comparison of total pressure contours at the duct entrance plane between the NACA inlet with a vortex generator and the standard NACA inlet. From Figure 11, it can be observed that the NACA inlet with a vortex generator has a higher total pressure than the standard NACA inlet. The vortex generator with a height of 64 mm attains the highest total pressure, resulting in the highest Ram recovery ratio among other configurations. Moreover, Figure 11 also indicates that the 64 mm height configuration reduces flow distortion at the duct entrance plane, leading to a more uniform airflow compared to the standard NACA inlet.

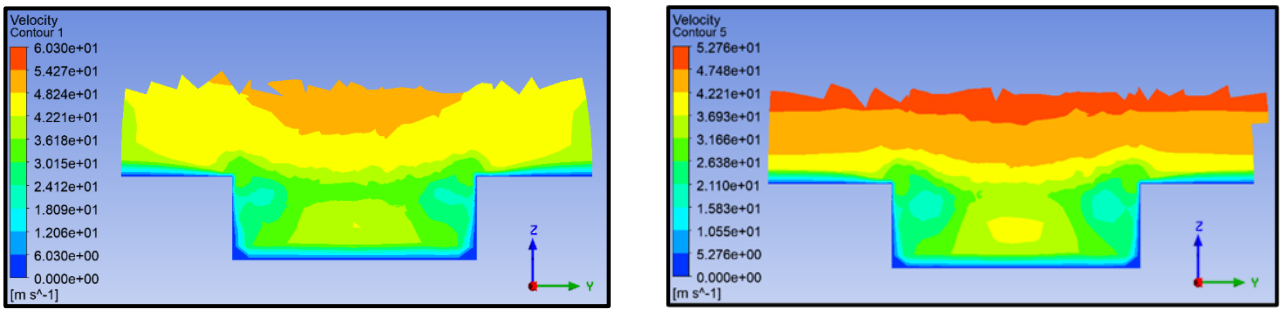

(a) (b)

Fig. 10. Velocity contour of the end section plane (a) with vortex generator *h* = 64 mm (b) standard

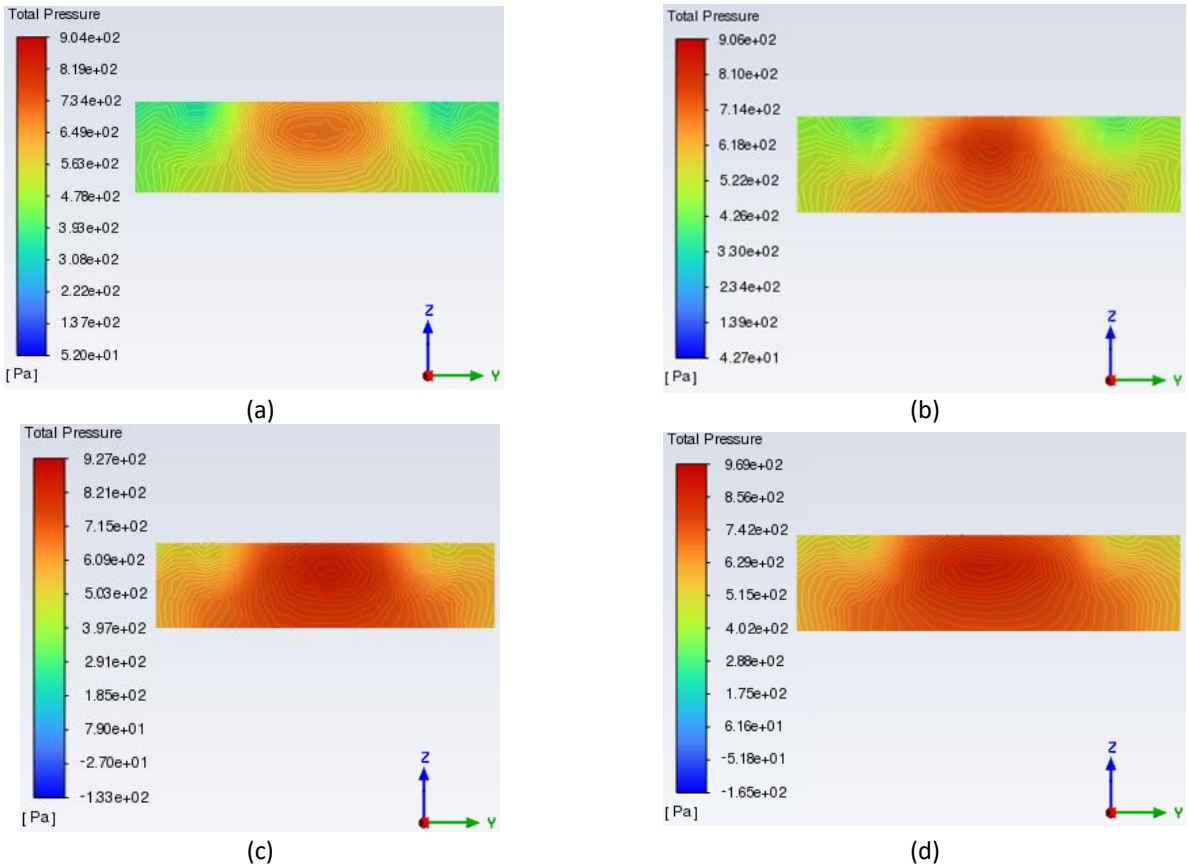

Fig. 11. Total pressure contour at NACA duct entrance (a) standard (b) VG *h* = 32 mm (c) VG *h* = 52 mm (d) VG *h* = 64 mm

The simulation results indicate that a vortex generator with a height matching the boundary layer thickness has the highest performance improvement, consistent with the findings of research on the effect of vortex generator height conducted by Li *et al.,* [23]. The research reveals that the kinetic energy in the vortex core height is ineffective for vortex generators with heights below the boundary layer thickness. The kinetic energy of the fluid increases logarithmically with the rise in vortex generator height. When the vortex generator height exceeds the boundary layer thickness, the kinetic energy remains unchanged. Hence, a vortex generator with a height equal to the boundary layer thickness is an ideal configuration for enhancing the kinetic energy in the boundary layer.

3.3 Effect of Vortex Generator Angle of Incidence

To observe the effects of the angle of incidence parameter, simulations with angle variations were conducted for a configuration with a vortex generator height of 64 mm and a spacing of 10 mm. Angle variations were performed from 12 degrees to 24 degrees with a 2-degree increment. Simulation results for angle variations on the Ram recovery ratio are shown in Figure 12(a). Figure 12(a) illustrates that the Ram recovery ratio increases with the angle's elevation. When the angle reaches a certain value, the Ram recovery ratio starts to decline. The highest Ram recovery ratio value, reaching 0.77878, is achieved at an angle of incidence of 20 degrees. Beyond 20 degrees, the Ram recovery ratio decreases, but the difference is not substantial. Simulation results for angle variations on the Mass flow ratio are presented in Figure 12(b). In Figure 12(b), it can be observed that the increase in Mass flow ratio corresponds to the increase in the angle of incidence, with a decrease in Mass flow ratio at angles of incidence greater than 18 degrees. The Mass flow ratio value

at an angle of incidence of 18 degrees is 0.71775, representing a 14.43% increase compared to the standard NACA inlet.

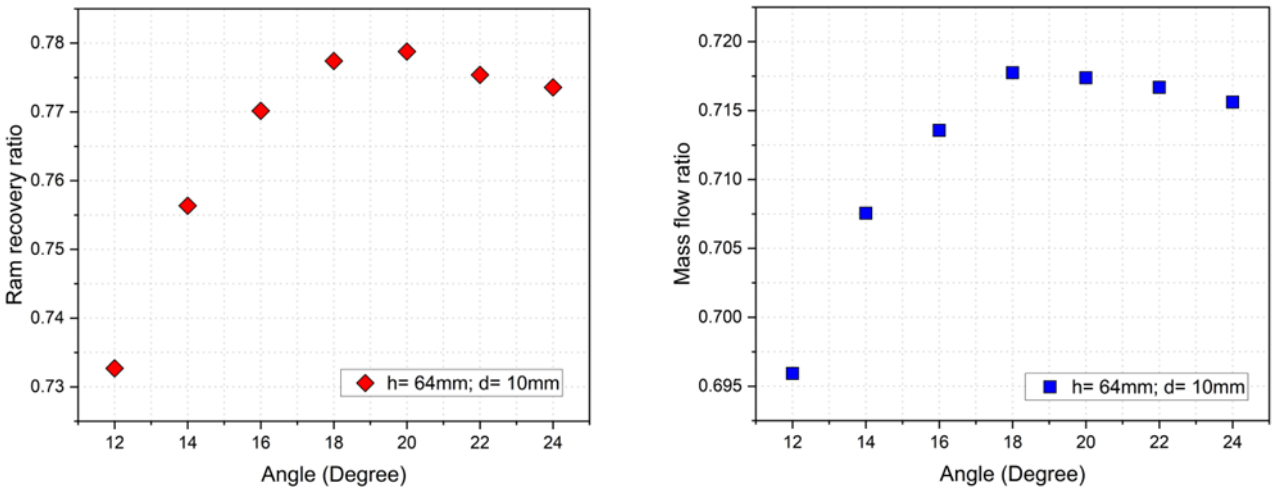

(a) (b)

Fig. 12. Effect of angle of incidence (a) Ram recovery ratio (b) Mass flow ratio

The reduction in boundary layer thickness with angle of incidence variations can be observed in Figure 13. As shown in Figure 13, the velocity contour on the NACA inlet with an 18-degree vortex generator exhibits a thinner boundary layer compared to the standard NACA inlet. The velocity contour values for the NACA inlet with a vortex generator in the middle towards the duct are greater than those for the standard NACA inlet. This boundary layer condition influences the total pressure values at the duct entrance region, as seen in Figure 14. It is evident that total pressure increases with an increase in the angle of incidence. However, when the angle of incidence becomes large, the total pressure values decrease. Total pressure at an angle of incidence of 18 degrees, as shown in Figure 14(c), is higher than the total pressure values at an angle of incidence of 24 degrees in Figure 14(d). Based on the comparison of Figure 14(c) and Figure 14(d), the total pressure values are not significantly different, and the flow structure is also relatively consistent.

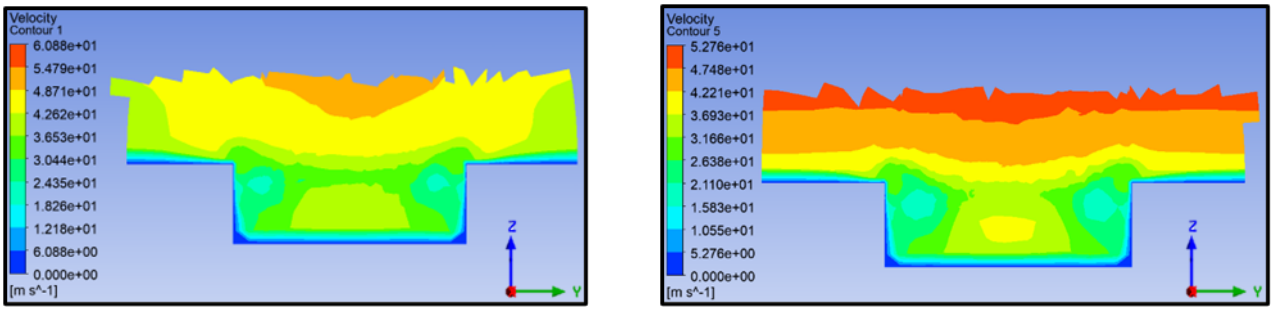

(a) (b)

Fig. 13. Velocity contour of the end section plane (a) with vortex generator β = 18 degree (b) standard

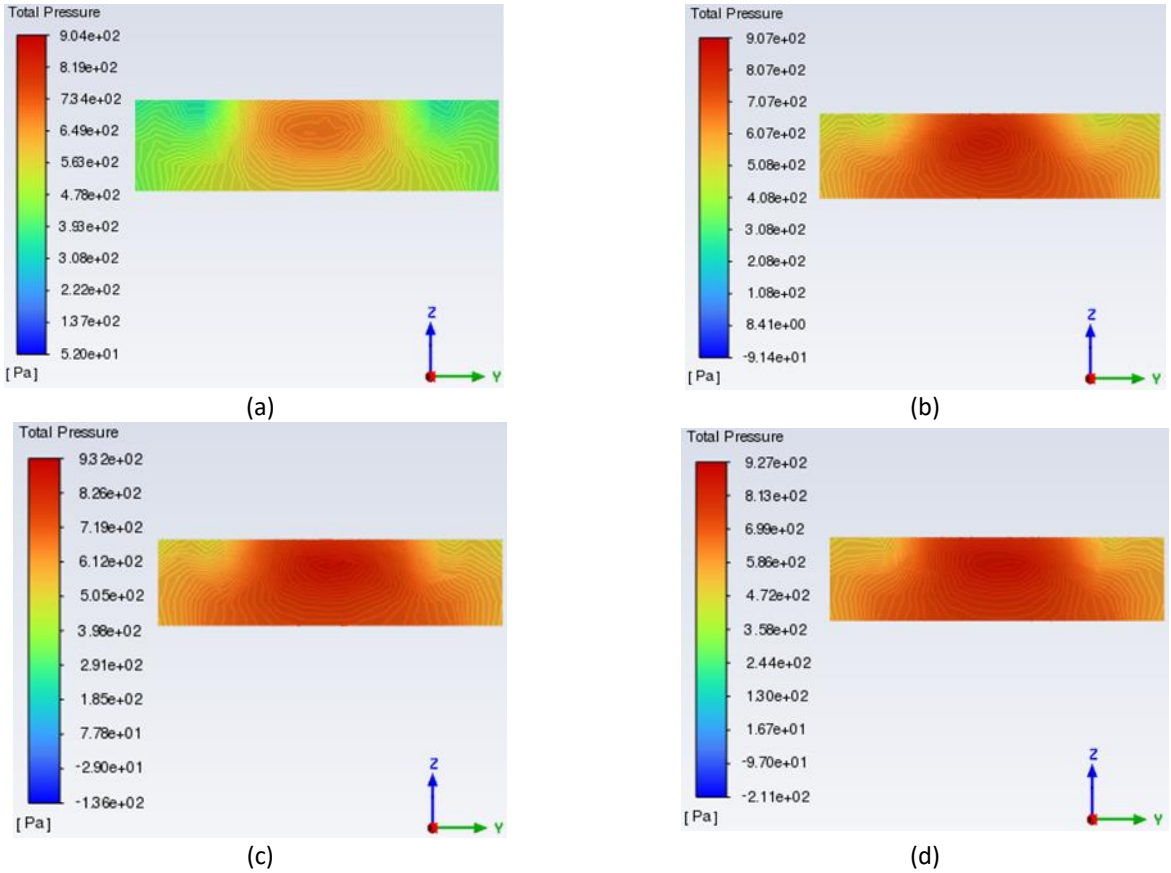

Fig. 14. Total pressure contour at NACA duct entrance (a) standard (b) VG β = 12 degree (c) VG β = 18 degree (d) VG β = 24 degree

The upward trend in Ram recovery and Mass flow ratio values with an increase in the angle of incidence, followed by a decrease after reaching a certain angle, can be attributed to several factors, including the intensity of the generated vortex. Li *et al.,* [24] in their study on the effect of the installation angle of vortex generators, found that as the installation angle is raised, the vortex strength increases until the vortex core eventually collapses. The configuration of the installation angle determines the intensity of the generated vortex. Therefore, there are effective streamwise distances for the use of vortex generators with a specific angle as flow control. In the case of the NACA inlet, the use of a 20-degree angle of incidence for the vortex generator proves to be highly effective in improving the performance of the NACA inlet.

3.4 Effect of Vortex Generator Spacing

The simulation conducted to determine the effect of vortex generator spacing involved variations in spacing ranging from 5 to 50 mm. The configuration was set with a vortex generator height of 64 mm and an angle of incidence of 20 degrees. The simulation results with spacing variations are shown in Figure 15. In Figure 15(a), it is evident that increasing the spacing will enhance the Ram recovery ratio. However, after reaching a certain spacing, the Ram recovery ratio will decrease. The decline occurs at spacing values greater than 20 mm. At a spacing of 20 mm, the obtained Ram recovery ratio is 0.78118, representing a 31.23% increase from the standard NACA inlet. The Ram recovery ratio values at spacing 30 mm and 50 mm are 0.77982 and 0.77617, respectively. Both values are lower than the value at spacing of 20 mm. Figure 15(b) shows the trend in Mass flow ratio, where the value increases up to a spacing of 20 mm and decreases as the spacing is enlarged. The highest Mass flow

ratio value, 0.7196, is achieved at a spacing of 20 mm. The vortex generator configuration with *h* = 64 mm, β = 20 degrees, and *d* = 20 mm results in the highest Ram recovery enhancement among other configurations, reaching 31.23%. This increase in the Ram recovery ratio is lower than the findings of the study by Perez *et al.,* [7] who used delta-type vortex generators. In their study, the Ram recovery ratio reached an increase of up to 53% with delta-type vortex generator configurations with support. Apart from the high-performance enhancement, there is an impact in the form of an 80% increase in drag coefficient.

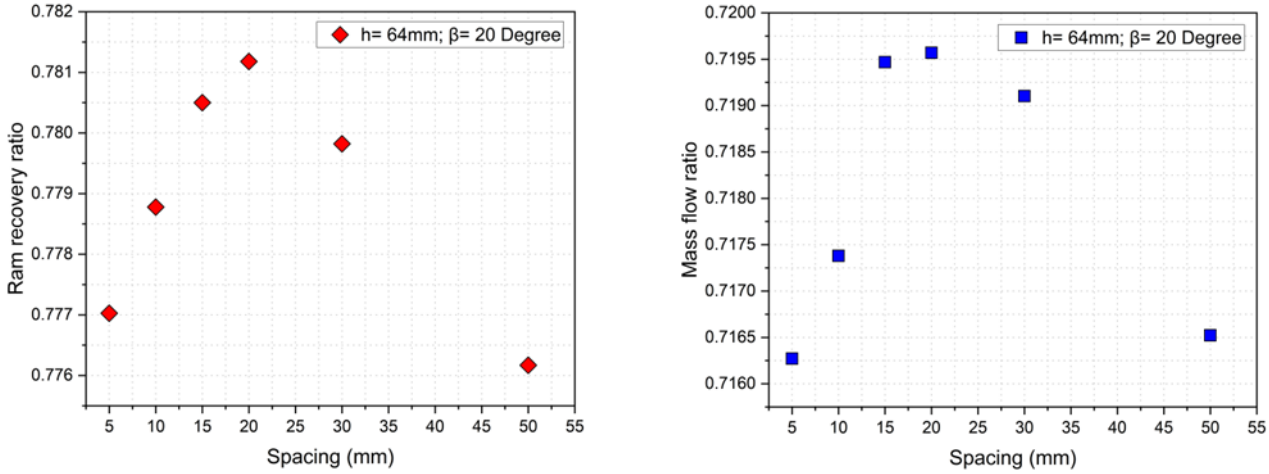

(a) (b)

Fig. 15. Effect of spacing (a) Ram recovery ratio (b) Mass flow ratio

Comparison of boundary layer thickness between the standard NACA inlet and the NACA inlet with various vortex generator spacings can be observed in Figure 16. Figure 16 indicates that the NACA with varying vortex generator spacings has a lower thickness at the bottom of the inlet compared to the standard NACA inlet. In the duct entrance plane, as shown in Figure 17, differences in total pressure can be seen, with higher total pressure values observed for the vortex generator with a spacing of 20 mm. In the configuration with a spacing of 50 mm, it is evident that the level of flow distortion is greater than in the 20 mm spacing configuration. This flow non-uniformity results in lower performance in the 50 mm spacing configuration compared to the 20 mm spacing configuration.

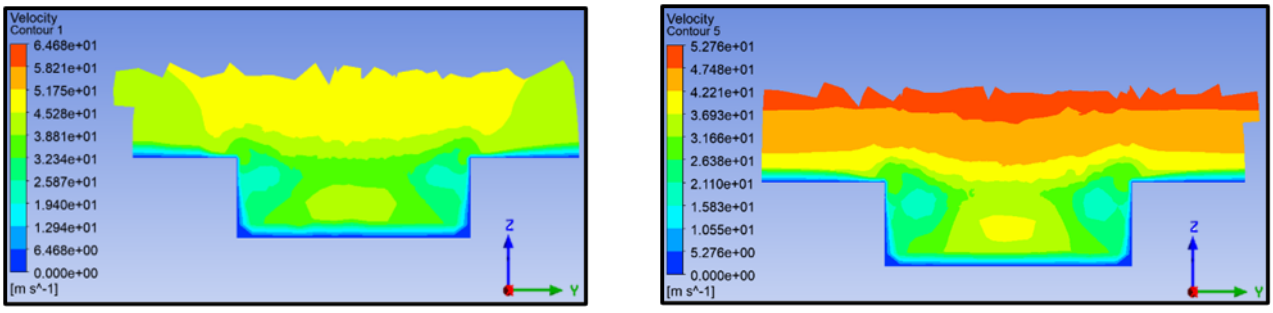

(a) (b)

Fig. 16. Velocity contour of the end section plane (a) with vortex generator *d* = 20 mm (b) standard

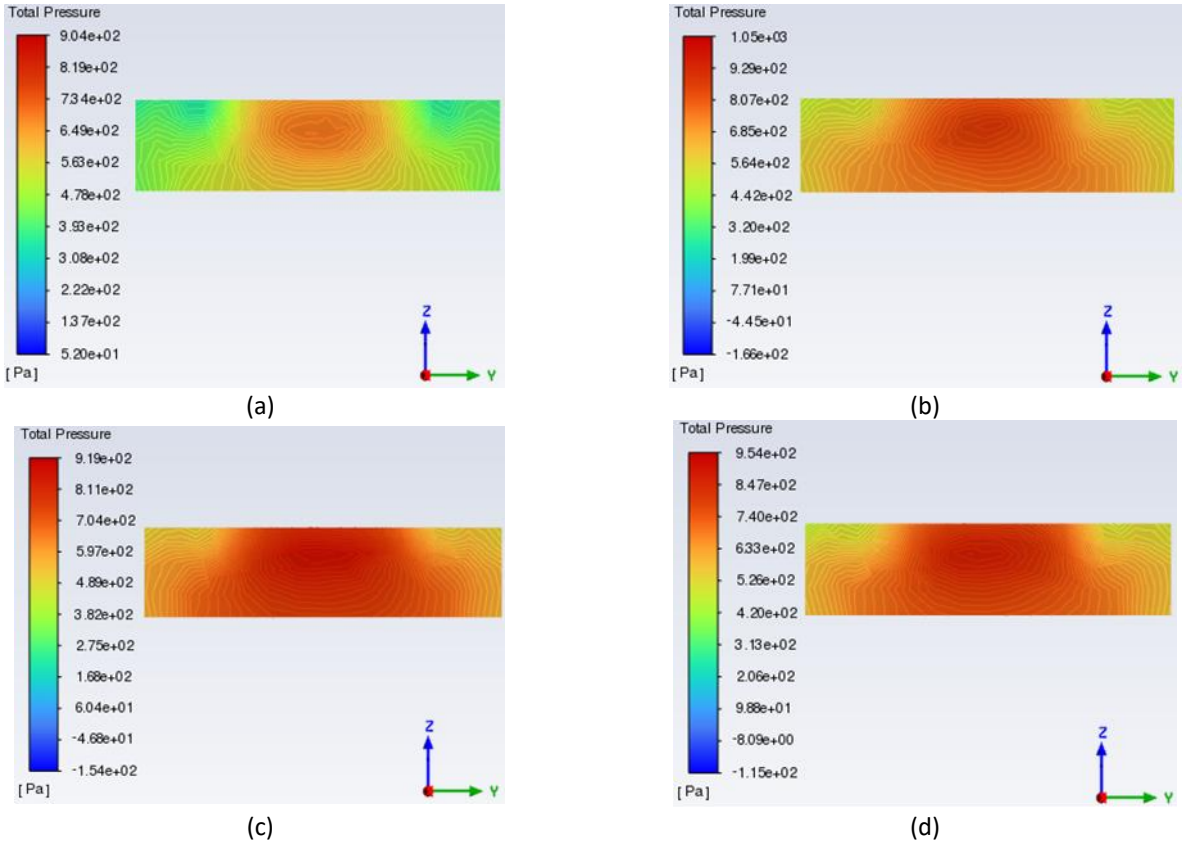

Fig. 17. Total pressure contour at NACA duct entrance (a) standard (b) VG *d* = 15 mm (c) VG *d*= 20 mm (d) VG *d* = 50 mm

With variations in vortex generator spacing, the values of Ram recovery and Mass flow ratio will increase until reaching their peak values and decrease significantly afterward. Based on the research by Li *et al.,* [25] low vortex generator spacing will cause the generated vortices to carry only a small portion of kinetic energy from the freestream flow to the vicinity of the wall. This is because the development of vortices generated by the vortex generator is impeded. In the case of using vortex generators in the NACA inlet, the development of vortices may be hindered at low spacing. As the vortex generator spacing increases, the generated vortices develop and effectively enhance the performance of the NACA inlet until a certain point. When the spacing is increased beyond the point of peak performance, the performance of the NACA inlet decreases because the distance between two vortices becomes unbalanced with the vortex radius, reducing the effective range of the vortices.

4. Conclusions

The performance of the NACA inlet is determined by the boundary layer thickness at the upstream inlet. The study aimed to investigate the influence of geometric parameters of the vortex generator on the performance of the NACA inlet. CFD simulations were conducted in the study of the vortex generator placed at a specific distance from the NACA inlet with variations in geometric parameters. The geometric parameters varied including height, angle of incidence, and spacing of the vortex generator. Simulations were performed on 16 configurations to understand the influence of each parameter. To evaluate the performance of the NACA inlet, parameters such as Ram recovery and Mass flow ratio were employed.

Based on the CFD simulations, it can be concluded that the configuration with h = 64 mm, β = 20 degrees, and d = 20 mm yields the most significant improvement in the performance of the NACA

inlet. The Ram recovery ratio achieved is 0.7812, and the Mass flow ratio is 0.7196. Both values represent an increase of 31.23% for the Ram recovery ratio and 14.72% for the Mass flow ratio compared to the standard NACA inlet. The simulation results further reveal that aligning the height of the vortex generator with the local boundary layer thickness is most effective in enhancing the NACA inlet performance. Additionally, increasing the angle of incidence enhances the inlet performance until reaching a peak at a certain angle, beyond which further increases become ineffective. Regarding vortex generator spacing, performance initially suffers at small spacings but improves as the spacing increases up to an optimal distance. However, increasing the spacing beyond optimal distance decreases the inlet performance due to a decline in the enhancement of fluid kinetic energy in the boundary layer.

Future work should involve adding variations to other parameters of the vortex generator to enhance the performance of the NACA inlet. Parameters such as increasing the number of vortex generators need further investigation. By increasing the number of vortex generators, it is expected to enhance vortex intensity and the effectiveness of the vortex generator. Validation of the numerical study results needs to be performed through measurements using accurate equipment in a wind tunnel experiment.

Acknowledgment
This research was not funded by any grant.

References

[1] Rütten, Markus, Lars Krenkel, and Malte Freund. "Parametric design, comparison and evaluation of air intake types for bleedless aircraft." In *39th AIAA Fluid Dynamics Conference*, p. 3902. 2009. https://doi.org/10.2514/6.2009-3902

[2] Devine, Raymond, John Watterson, and Richard Cooper. "An investigation into improving the performance of low speed auxiliary air inlets using vortex generators." In *20th AIAA applied aerodynamics conference*, p. 3264. 2002. https://doi.org/10.2514/6.2002-3264

[3] Devine, R. J., J. K. Watterson, and R. K. Cooper. "Performance improvement of flush, parallel walled auxiliary intakes by means of vortex generators." In *Proceedings of the 24th International Congress for Aeronautical Sciences*. 2004.

[4] Rütten, Markus, and Holger Wendland. "Performance enhancement of auxiliary air intakes using vortex generators." In *50th AIAA Aerospace Sciences Meeting including the New Horizons Forum and Aerospace Exposition*, p. 57. 2012. https://doi.org/10.2514/6.2012-57

[5] Küçük, Umut C., Özgür U. Baran, and Oguz Uzol. "Passive flow control in boundary layer ingesting semi submerged inlet." In *51st AIAA/SAE/ASEE Joint Propulsion Conference*, p. 3803. 2015. https://doi.org/10.2514/6.2015-3803

[6] Huang, Cong-Lei, Ren Dai, and Zong-Long Wang. "Effects of upstream vortex generators on the intake duct performance for a waterjet propulsion system." *Ocean Engineering* 239 (2021): 109838. https://doi.org/10.1016/j.oceaneng.2021.109838

[7] Pérez, César Celis, Sandro Barros Ferreira, Luís Fernando Figueira da Silva, Antônio Batista de Jesus, and Guilherme Lara Oliveira. "Computational study of submerged air inlet performance improvement using vortex generators." *Journal of aircraft* 44, no. 5 (2007): 1574-1587. https://doi.org/10.2514/1.25036

[8] Sun, Shu, Hui-Jun Tan, and Chen-Xi Wang. "Submerged inlet performance enhancement using a unique bump-shaped vortex generator." *Journal of Propulsion and Power* 32, no. 5 (2016): 1275-1280. https://doi.org/10.2514/1.B36085

[9] Saheby, Eiman B., Xing Shen, Guoping Huang, and Anthony P. Hays. "Flow structure of the ridge integrated submerged inlet." *Aerospace Science and Technology* 119 (2021): 107136. https://doi.org/10.1016/j.ast.2021.107136

[10] Xie, W. Z., S. Z. Yang, C. Zeng, K. Liao, R. H. Ding, L. Zhang, and S. Guo. "Effects of forebody boundary layer on the performance of a submerged inlet." *The Aeronautical Journal* 125, no. 1289 (2021): 1260-1281. https://doi.org/10.1017/aer.2021.8

[11] Mossman, Emmet A., and Lauros M. Randall. *An experimental investigation of the design variables for NACA submerged duct entrances*. No. NACA-RM-A7I30. 1948.

[12] Frick, Charles W., Wallace F. Davis, Lauros M. Randall, and Emmet A. Mossman. *An experimental investigation of NACA submerged-duct entrances*. No. NACA-ACR-5I20. 1945.
[13] Godard, Gilles, and Michel Stanislas. "Control of a decelerating boundary layer. Part 1: Optimization of passive vortex generators." *Aerospace science and technology* 10, no. 3 (2006): 181-191.. https://doi.org/10.1016/j.ast.2005.11.007
[14] Shlash, Bassam Amer Abdulameer, and Ibrahim Koç. "Turbulent fluid flow and heat transfer enhancement using novel Vortex Generator." *Journal of Advanced Research in Fluid Mechanics and Thermal Sciences* 96, no. 1 (2022): 36-52. https://doi.org/10.37934/arfmts.96.1.3652
[15] Lin, John C. "Review of research on low-profile vortex generators to control boundary-layer separation." *Progress in aerospace sciences* 38, no. 4-5 (2002): 389-420. https://doi.org/10.1016/S0376-0421(02)00010-6
[16] Biswas, Rupak, and Roger C. Strawn. "Tetrahedral and hexahedral mesh adaptation for CFD problems." *Applied Numerical Mathematics* 26, no. 1-2 (1998): 135-151. https://doi.org/10.1016/S0168-9274(97)00092-5
[17] Menter, Florian R., Martin Kuntz, and Robin Langtry. "Ten years of industrial experience with the SST turbulence model." *Turbulence, heat and mass transfer* 4, no. 1 (2003): 625-632.
[18] Fluent, A. N. S. Y. S. "Ansys fluent theory guide." Ansys Inc., USA 15317 (2011): 724-746.
[19] Bertin, John J., and Russell M. Cummings. *Aerodynamics for engineers*. Cambridge University Press, 2021. https://doi.org/10.1017/9781009105842
[20] American Institute of Aeronautics and Astronautics. *AIAA guide for the verification and validation of computational fluid dynamics simulations*. American Institute of aeronautics and astronautics., 1998.
[21] Coleman, Hugh W., and Fred Stern. "Uncertainties and CFD code validation." (1997): 795-803. https://doi.org/10.1115/1.2820713
[22] Li, Hualei, Lei Shi, and Kangyao Deng. "Research on the power recovery of diesel engines with regulated two-stage turbocharging system at different altitudes." *International Journal of Rotating Machinery* 2014 (2014). http://dx.doi.org/10.1155/2014/209084
[23] Li, Xinkai, Ke Yang, and Xiaodong Wang. "Experimental and numerical analysis of the effect of vortex generator height on vortex characteristics and airfoil aerodynamic performance." *Energies* 12, no. 5 (2019): 959. https://doi.org/10.3390/en12050959
[24] Li, Xin-Kai, Wei Liu, Ting-Jun Zhang, Pei-Ming Wang, and Xiao-Dong Wang. "Experimental and numerical analysis of the effect of vortex generator installation angle on flow separation control." *Energies* 12, no. 23 (2019): 4583. https://doi.org/10.3390/en12234583
[25] Li, Xin-kai, Wei Liu, Ting-jun Zhang, Pei-ming Wang, and Xiao-dong Wang. "Analysis of the effect of vortex generator spacing on boundary layer flow separation control." *Applied Sciences* 9, no. 24 (2019): 5495. https://doi.org/10.3390/app9245495